ELSEVIER

Thermochimica Acta 352–353 (2000) 213–221

thermochimica acta

www.elsevier.com/locate/tca

The behavior of water molecules in the most stable subgel phase of dimyristoylphosphatidylethanolamine–water system as studied by differential scanning calorimetry

Michiko Kodama*, Hidenori Kato, Hiroyuki Aoki

Department of Biochemistry, Okayama University of Science, 1-1 Ridai-cho Okayama 700-0005, Japan

Received 12 August 1999; received in revised form 12 October 1999; accepted 12 October 1999

Abstract

The number of water molecules in different bonding modes were estimated from ice-melting DSC curves for the most stable subgel phase of dimyristoylphosphatidylethanolamine (DMPE)–water system at different water contents, and used to prepare a water-distribution diagram up to a full hydration. By the present study, it was revealed that approximately 5 H_2O of water molecules per lipid present as members of the interlamellar water in the gel phase are excluded outside the bilayers during periods of thermal annealing for the conversion to the most stable subgel phase. The dehydrated subgel phase was found to involve 1 H_2O of the freezable interlamellar water per lipid, via which adjacent bilayers are linked. Furthermore, almost no interlamellar water was found in intrabilayer regions between the head groups of the present subgel phase, in contrast with approximately 2 H_2O of water molecules per lipid for the intrabilayer regions of the gel phase.

Keywords: DMPE; DSC; Subgel phase; Interlamellar water; Water-distribution diagram

1. Introduction

Phosphatidylethanolamine (PE), as well as phosphatidylcholine (PC), is a widely distributed phospholipid in biomembranes and constitutes their fundamental bilayer structure. Studies of lateral packings of lipid molecules and their interaction with water molecules in a bilayer are the subject of many investigators. In this connection, it has been revealed that dimyristoylethanolamine (DMPE)–water system is present in three phases in a solid-like state of lipid hydrocarbon chains [1–9]. To make clear this phenomenon, Fig. 1 shows a schematic diagram of relative enthalpy (ΔH) vs. temperature (t) curves previously reported by Kodama et al. [1]. The diagram indicates a low thermodynamic stability of the gel phase which is the most ordinary phase at temperatures of solid-like hydrocarbon chains. Thus, two phases, designated as L-, and H-subgel phases, are present in more stable states than the gel phase. Furthermore, it has been found by Kodama et al. [1] that the most stable H-subgel phase is three-dimensional bilayer stacks, but the amount of water incorporated in regions between the adjacent bilayers is fairly less, compared with the gel phase.

In the present study, the number of water molecules in different bonding modes was estimated from ice-

* Corresponding author. Tel.: +81-86-252-3161; fax: +81-86-255-7700.

0040-6031/00/$ – see front matter
PII: S0040-6031(99)00469-4

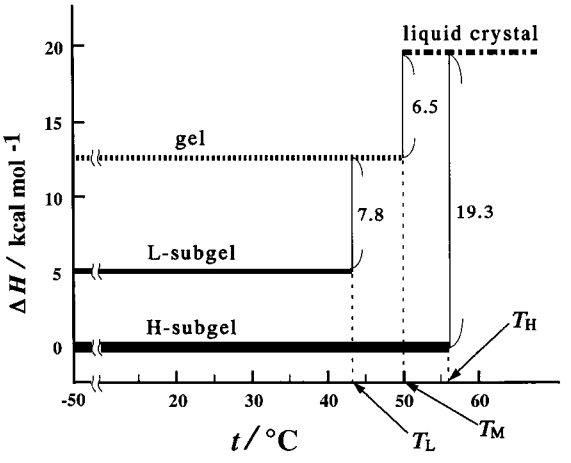

Fig. 1. Schematic diagram of relative enthalpy (ΔH) vs. temperature (t) curves for DMPE–water system [1]. The diagram was constructed on the basis of transition temperatures and transition enthalpies obtained by DSC. Two subgel phases are distinguished by symbols, L and H, depending on whether their transition appear at temperatures lower or higher than the gel-to-liquid crystal phase transition.

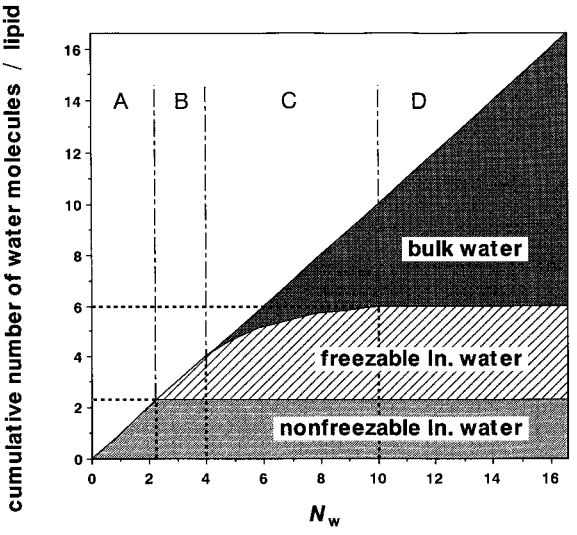

Fig. 2. Diagram of water distribution for the gel phase of DMPE–water system [10]. A cumulative number of water molecules present in nonfreezable interlamellar and freezable interlamellar and bulk waters per lipid is plotted against a water/lipid molar ratio (N_w). The diagram are classified into four categories of A, B, C and D. The category C is a specific region, designated as a pre-region [10].

melting DSC curves for the most stable H-subgel phase of DMPE–water system at different water contents and a distribution diagram for water molecules present in nonfreezable and freezable interlamellar waters and bulk water was prepared over the water content up to a full hydration. By comparing a resultant diagram of H-subgel phase with that of the gel phase previously reported by Kodama et al. [10], the present study will discuss the following problems: (i) a difference in the water distribution between H-subgel and gel phases and (ii) the role of water molecules in the conversion of the gel to H-subgel phases attained by a thermal annealing.

2. Experimental

Material: 1,2-Dimyristoyl-*sn*-glycero-3-phosphatidylethanolamine was purchased from Sigma and used without further purification.

Preparation of gel sample: As H-subgel phase is obtained by annealing thermally the gel phase under specific conditions, the gel sample of DMPE–water mixture was first prepared by an addition of a desired amount of water to a dehydrated lipid by using a microsyringe. The water content of the sample was ascertained by weighing the sample and the cell by microbalance. As a water-distribution diagram (see Fig. 2) for the gel phase previously reported by Kodama et al. [10] is grouped into four categories A, B, C and D depending on water content, the water contents of the present samples were adjusted to desired values which belong to four categories, respectively. All the samples were annealed by repeating thermal cycling at temperatures above and below the lipid transition to the liquid crystal phase to ensure homogeneous mixing. The thermal cycling was repeated at least three times, until the same transition peak was attained. After that, the samples were cooled to -60°C for the differential scanning calorimetry (DSC). After the DSC, the weight of the sample and the cell was rechecked by microbalance.

Preparation of H-subgel sample: The conversion of the gel to H-subgel phases was performed according to a procedure based on two steps of annealing at different temperatures, previously established by Kodama et al. [1], that is, the gel sample was kept at around -60°C for at least 5 h (nucleation), and then

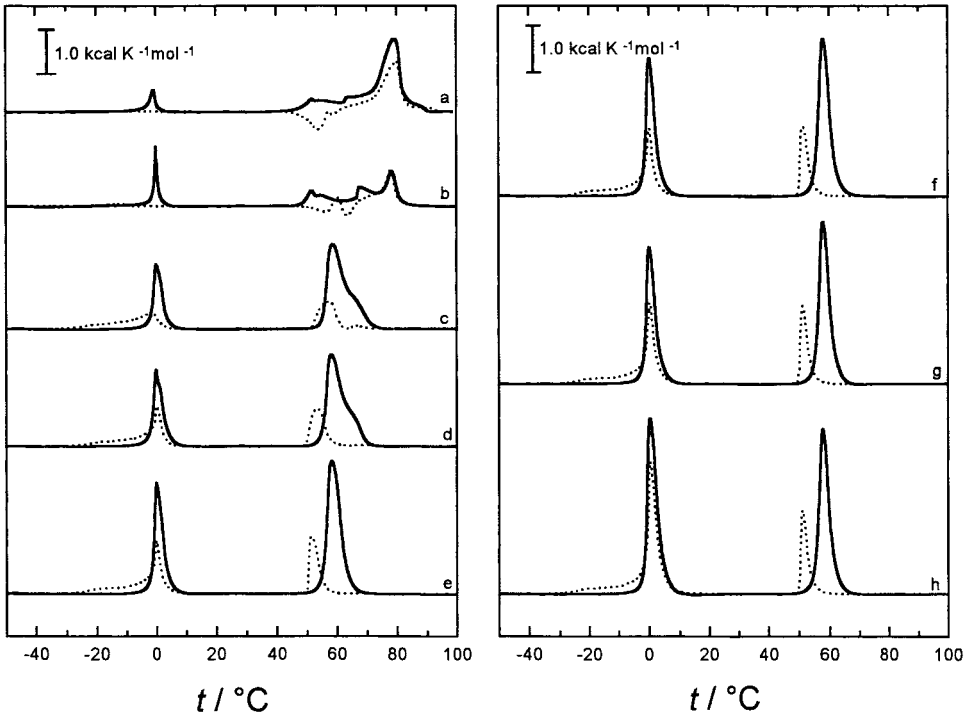

Fig. 3. A series of comparisons of thermal behavior for pair samples, annealed and nonannealed, at the same water content for DMPE–water system. Annealed samples (H-subgel phase) are shown by solid lines and nonannealed samples (gel phase) by dotted lines. Water content (wt.%): a, 5.1 (1.9); b, 8.1 (3.1); c, 12.1 (4.8); d, 15.0 (6.2); e, 18.0 (7.8); f, 20.0 (8.8); g, 22.0 (9.9); h, 28.0 (13.7). The values in brackets show the corresponding N_w.

at a temperature (about 47°C) just below the gel-to-liquid crystal phase transition for about 24 h (nuclear growth). However, the samples at low water contents of $N_w < 4$ were annealed at temperatures of an exothermic phenomenon observed in a heating DSC (see Fig. 3).

Differential scanning calorimetry (DSC): DSC was carried out with a Mettler TA-4000 apparatus by placing the sample in a high-pressure crucible (pressure resistant to 10 MPa) and heating it from −60°C to temperatures above the transition to the liquid crystal phase at a rate of 1°C/min.

3. Definitions and determination of the number of water molecules

The water molecules in lipid–water systems are classified into three types, nonfreezable interlamellar, freezable interlamellar and bulk waters. The nonfreezable interlamellar water is most likely to exist in regions between adjacent lipid head groups in an intrabilayer [11]. Presumably, this type of water molecule cannot participate in the formation of ice-like hydrogen bonds among the neighboring water molecules, even though cooled to extremely low temperatures. Furthermore, if the water molecule existing nearest the surface of bilayer is bound to lipid head groups as tightly as impossible to form the hydrogen bonds with the neighboring water molecules on cooling, it could be taken as the nonfreezable water. All the nonfreezable water in the present system is found in regions between lamellae, and so designated as nonfreezable interlamellar water, in order to distinguish it from the freezable water between lamellae. On the other hand, the freezable water is present in two types designated as freezable interlamellar water and bulk water, respectively. The freezable interlamellar water,

although present in the interbilayer region, keeps enough freedom to form the ice-like hydrogen bonds on cooling. However, the ice-melting DSC curve for this freezable water is observed to extend over the wide temperature range from around −40°C to as close as 0°C. The bulk water exists outside the bilayers and the ice-melting behavior is close to that of a hexagonal ice derived from the so-called free water.

A correlation in the number of these water molecules at a desired water content is given by the following equation:

$$N_T = N_{I(nf)} + N_{I(f)} + N_B \quad (1)$$

where N_T is the total number of water molecules per lipid molecule and $N_{I(nf)}$, $N_{I(f)}$ and N_B the number per lipid of each water molecule present in nonfreezable interlamellar, freezable interlamellar and bulk waters. When a molar mass is used, N_T is the molar number of water added per mol of lipid and equal to a water/lipid molar ratio, N_w, of a sample. In the present study, N_T and N_w are treated separately. By assuming that the bulk water behaves as free water and also using the known melting enthalpy of the hexagonal ice, 1.436 kcal/(mol of water), Eq. (1) is replaced by

$$1.436(N_T - N_B) = 1.436(N_{I(nf)} + N_{I(f)}) \quad (2)$$

In Eq. (2), each term is expressed in a unit of kcal/(mol of lipid). The first term of 1.436 N_T is a theoretical ice-melting enthalpy, ΔH_T, based on the assumption that N_T moles of water molecules are all present as the bulk water. The second term of 1.436 N_B is an experimental ice-melting enthalpy, ΔH_B, for N_B moles of water molecules actually present as the bulk water and determined from ice-melting DSC curve. On this basis, Eq. (2) is given by

$$\Delta H_T - \Delta H_B = 1.436(N_{I(nf)} + N_{I(f)}) \quad (3)$$

On the basis of Eq. (3), the number of whole interlamellar water molecules, $N_I = N_{I(nf)} + N_{I(f)}$, at each N_w was calculated from $(\Delta H_T - \Delta H_B)/1.436$.

For estimations of each of $N_{I(f)}$ and $N_{I(nf)}$ consisting of N_I, it is required to measure the ice-melting DSC curve over the entire water content up to a full hydration. This method is based on the assumption that the water added to a sample is preferentially interposed into regions between lipid head groups until a limiting, maximum amount of the nonfreezable interlamellar water is reached. $N_{I(nf)}$ is estimated from a plot against N_w of the ice-melting enthalpy for the freezable interlamellar water, $\Delta H_{I(f)}$, determined from ice-melting DSC curve (see Fig. 7), and then $N_{I(f)}$ is calculated from $N_I - N_{I(nf)}$ (details are discussed in the text).

As discussed above, N_B is estimated from ice-melting DSC curve. So, it is required to determine ΔH_B as accurately as possible. From this viewpoint, the ice-melting DSC curve was separated into at least two components for the freezable interlamellar and bulk waters by a deconvolution analysis, because both components overlap each other at the foot. The deconvolution was performed according to a computer program for a multiple Gaussian curve analysis. In the present deconvolution, the ice-melting DSC curve was deconvoluted into the minimum number of components, by applying the following conditions that (i) a theoretical curve given by the sum of individual deconvoluted curves is best fitted to the experimental DSC curve; and (ii) both the half-height width and the midpoint temperature of each deconvoluted curve are maintained almost constant throughout all the deconvolutions for varying water contents. Standard deviations of the present deconvolutions are 0.1–0.3 kcal K^{-1} mol^{-1}, which correspond to approximately ±0.2 H_2O per lipid.

4. Results and discussion

Phase transition behavior of lipid: Fig. 3 shows a series of comparisons between thermal behavior of the annealed (solid lines) and nonannealed samples (dotted lines) at the same water content in DMPE–water system. In our previous study [10], it has been revealed that the thermal behavior of lipid phase transition for the nonannealed samples are grouped into three types depending on water contents, $N_w < 4$ (categories A and B), $4 \leq N_w < 10$ (category C), and $N_w \geq 10$ (category D) shown in Fig. 2. In Fig. 3, similar behavior depending on water content is observed for the transition peak of the present annealed samples. Thus, as is shown in Fig. 3a and b, the annealed samples for $N_w < 4$ exhibit the transition peak of composite components, similarly to the nonannealed samples at the same water contents. Such a transition phenomenon have been already reported by Kodama et al. [12] for the transition of the hydrated

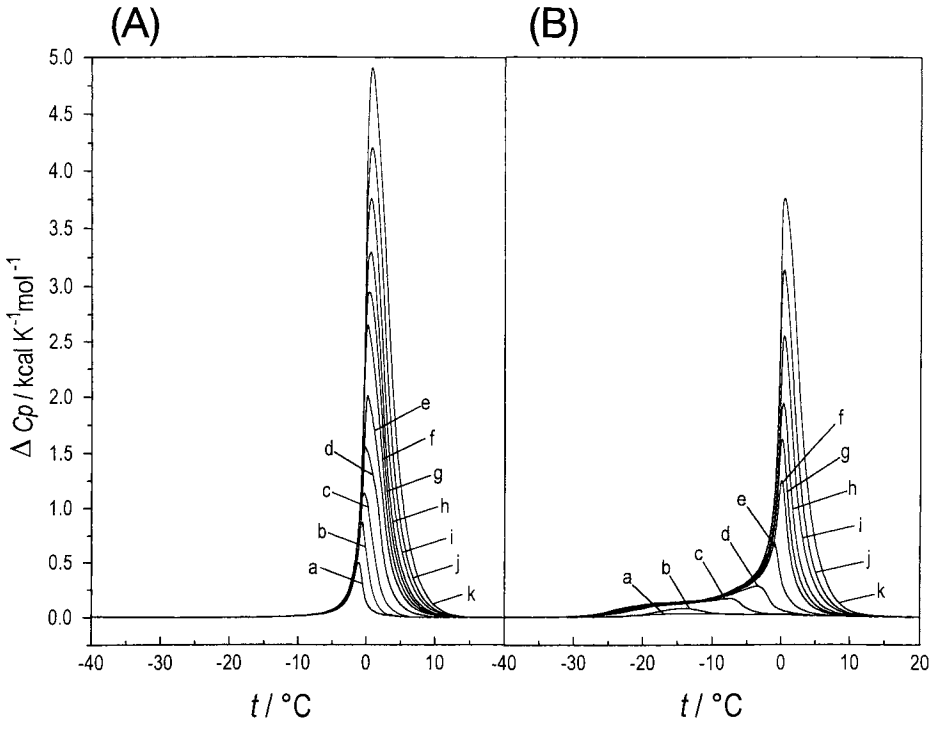

Fig. 4. A series of ice-melting DSC curves of varying water contents for H-subgel phase (A) of DMPE–water system, compared with results for the gel phase (B) at the same water content. Water content (wt.%): a, 5.1 (1.9); b, 8.1 (3.1); c, 10.0 (4.0); d, 12.1 (4.8); e, 15.0 (6.2); f, 18.0 (7.8); g, 20.0 (8.8); h, 22.0 (9.9); i, 25.0 (11.7); j, 28.0 (13.7) ; k, 32.0 (16.6). The values in brackets show the corresponding N_w.

crystalline phase to liquid crystal phase at low water contents of a lipid–water mixture. Therefore, the present annealed samples are also found to exist in composite hydrated crystals in different hydration numbers in the low water content region. For $4 \leq N_w < 10$, as shown in Fig. 3c–f, the transition peaks for the nonannealed and annealed samples are almost single, but with an increase in water content, they converge to limiting, fixed peaks observed for $N_w \geq 10$ (Fig. 3g and h), respectively, which have been generally accepted as the transition peaks of gel-to-liquid crystal and H-subgel-to-liquid crystal phases [1,5,7,8].

Ice-melting behavior: In Fig. 4, a series of the ice-melting DSC curves at different water contents are compared between the annealed (A) and nonannealed samples (B) in an enlarged scale. In this figure, all the melting curves for the annealed samples are shown to overlap in a similar shape, even for $N_w < 4$ where the composite phases coexist. Accordingly, the phases at the low water contents for the annealed samples were treated as ones analogues to H-subgel phase observed at the higher water contents. It is understandable that the ice-melting curves for the annealed samples are derived from the freezable water present in H-subgel phase because they are followed by the transition of H-subgel-to-liquid crystal phases, as shown in Fig. 3. Similarly, the melting curves for the nonannealed samples are assigned to the freezable water present in the gel phase [10]. The melting curves for the annealed subgel samples shown in Fig. 4A shows a growth of the sharp component at around 0°C and simultaneously a disappearance of the broad component at the lower temperatures, compared with those for the nonannealed gel samples in Fig. 4B. Details are as follows: Although no ice-melting peak is observed for the gel samples at $N_w = 1.9$ (category A in Fig. 2), as shown in Fig. 4B(a), a small, sharp melting peak at around 0°C is detected for the subgel sample at the same water content. This suggests a conversion of the

nonfreezable interlamellar water in the gel phase to the bulk water in the subgel phase. As shown in Fig. 4B(b), the gel sample at $N_w = 3.1$ (category B in Fig. 2) exhibits only a faint, broad melting peak at temperatures below 0°C, but an enlarged, sharp melting peak shown in Fig. 4A(b) is observed for the subgel sample at the same water content. Such a difference in the ice-melting curve is more clearly recognized in Fig. 4 for the samples at higher water contents (categories C and D in Fig. 2). Thus, the broad peak extending over the wide temperature range below 0°C in the gel phase is replaced by the sharp peak at around 0°C in the subgel phase, indicating a change from the freezable interlamellar to bulk waters.

Estimation of water molecules and water-distribution diagram: As is shown in Fig. 4A, the onset temperature of sharp ice-melting peak for the subgel phase is approximately −8°C. Therefore, it is reasonable to consider that the ice-melting curve involves at least one component other than the component for the bulk water which occupies a large portion of the curve. From this viewpoint, to estimate ΔH_B given in Eq. (3) for the present subgel phase, all the ice-melting curves shown in Fig. 4A were deconvoluted according to the above-described method. In Fig. 5, results of the deconvolution analysis are shown for two subgel samples at different water contents, compared with those for the gel samples at the corresponding water contents. In Fig. 5A(a) and B(a) for the subgel phase, the ice-melting curves are shown to be deconvoluted into two components, curves III and IV, derived from the freezable interlamellar and bulk waters, respectively. This indicates the lack of two other components of deconvoluted curves I and II for the freezable interlamellar water observed for the gel phase in Fig. 5A(b) and B(b).

On the other hand, the enthalpy change of the deconvoluted curve IV shown in Fig. 5 gives ΔH_B in Eq. (3), and so ΔH_B for the subgel phase was determined at each water content from the enthalpy change of the deconvoluted curve IV. In Fig. 6, resultant ΔH_B is plotted against N_w, compared with a theoretical curve for ΔH_T given in Eq. (3). Furthermore, for comparison, ΔH_B curve for the gel phase [10] is also shown in Fig. 6. In this figure, for $N_w \geq 10$, the ΔH_B curve for the subgel phase, as well as that for the gel phase, is almost parallel to the straight ΔH_T line. This indicates that the enthalpy difference, $\Delta H_T - \Delta H_B$, given in Eq. (3) is equal for $N_w \geq 10$, so that N_I ($= N_{I(nf)} + N_{I(f)}$) is the same above this N_w. Thus, the amount of whole (nonfreezable plus freezable) interlamellar water for the subgel phase is reveled to reach a maximum at around $N_w = 10$, similarly to the gel phase [10]. The limiting maximum amount of the interlamellar water for the subgel phase can be determined graphically by extrapolating the linear ΔH_B (H-subgel) line for $N_w > 10$ to a lower N_w. Thus, the extrapolated ΔH_B (H-subgel) line shown by dotted lines intersects the abscissa at $N_w = 1.3$, so that N_I of the subgel phase is estimated to be 1.3 ± 0.2 H_2O per lipid for $N_w \geq 10$. This value is fairly smaller than the corresponding value (6.0 ± 0.2) for the gel phase determined by the same method. For $N_w < 10$, N_I was estimated from $(\Delta H_T - \Delta H_B)/1.436$ given by Eq. (3).

Next, each of $N_{I(nf)}$ and $N_{I(f)}$ was estimated from the resultant N_I. The enthalpy change of deconvoluted curve III for H-subgel phase shown in Fig. 5A(a) and B(a) gives the ice-melting enthalpy, $\Delta H_{I(f)}$, for the freezable interlamellar water of this phase. To detect a water content where the freezable interlamellar water appears for the first time, values of $\Delta H_{I(f)}$ for H-subgel phase were plotted against N_w and a polynominal curve best fitted to nine points for $N_w < 10$ was obtained. A resultant polynominal function was expressed by fifth orders with a standard deviation of 0.026 and intersected the abscissa at approximately $N_w = 0.3$. The functions above fifth orders showed larger standard deviations and those below the orders gave negative values for the N_w at the intersection point. In Fig. 7, the $\Delta H_{I(f)}$ curve for the subgel phase is compared with that for the gel phase given by the summation of the individual enthalpy changes of deconvoluted curves I, II and III shown in Fig. 5A(b) and B(b). Therefore, 0.3 ± 0.2 H_2O per lipid correspond to the maximum number of water molecules for the nonfreezable interlamellar water of H-subgel phase. However, considering an uncertainty for the $\Delta H_{I(f)}$ curve obtained by a polynominal curve fit, it may be suggested that there is almost no nonfreezable interlamellar water for the present subgel phase. This is contrasted with 2.3 ± 0.2 H_2O per lipid for the corresponding water molecules of the gel phase.

$N_{I(nf)}$, $N_{I(f)}$ and N_B given in Eq. (1) were estimated at each N_w and details of the estimations are summarized in Table 1. In this Table, the value of 0.3 ± 0.2 H_2O/

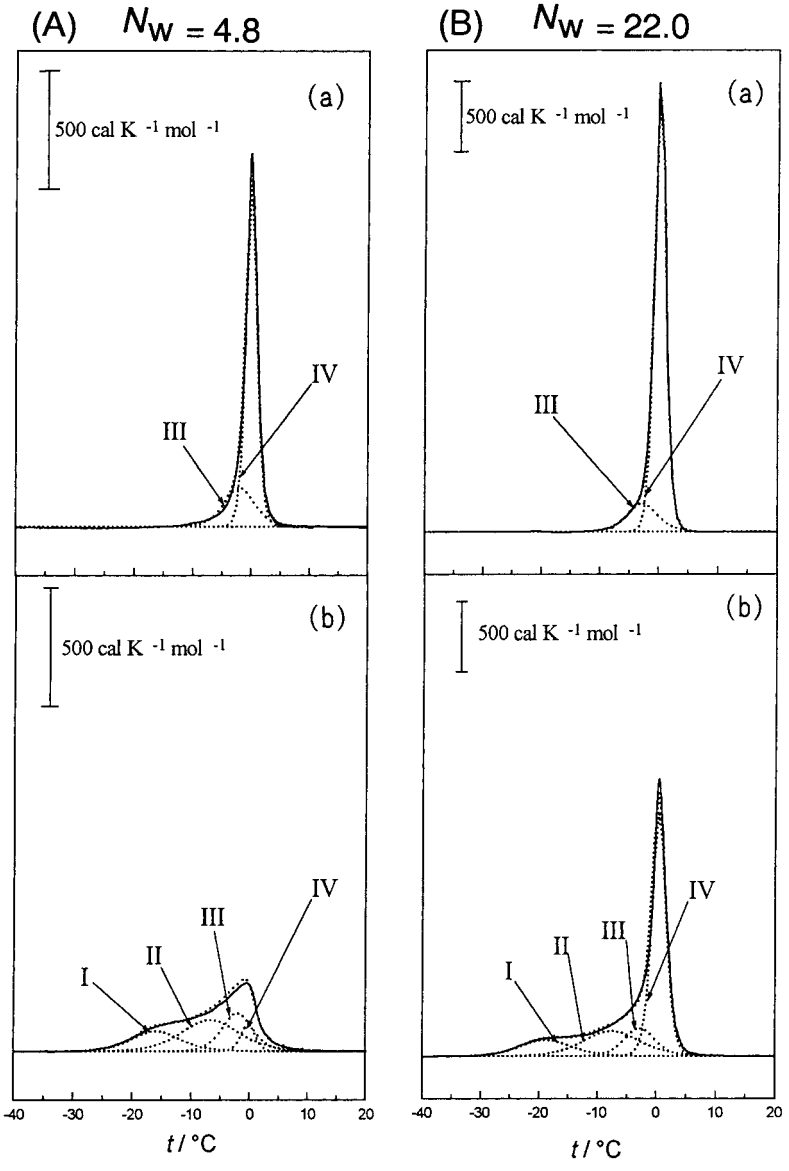

Fig. 5. Deconvolution analysis of ice-melting DSC curves for (a) H-subgel phase of DMPE–water system, compared with results for (b) the gel phase at the same water content. Water content (wt.%): A, 12.1 (4.8); B, 22.0 (9.9). The values in brackets show the corresponding N_w. Deconvoluted curves and their sum (theoretical curve) are shown by dotted lines and DSC curves by solid lines.

lipid estimated by our previous method [10] has been used as the maximum number of the nonfreezable interlamellar water molecules. Resultant $N_{I(nf)}$, $N_{I(f)}$ and N_B were used to prepare a diagram of water-distribution for the subgel phase and the diagram is shown in Fig. 8. By comparing with the diagram for the gel phase shown in Fig. 2, a fairly smaller amount of the interlamellar water is obvious for the subgel phase. Thus, the fully hydrated H-subgel phase involves 0.3 ± 0.2 H_2O of the nonfreezable interlamellar water and 1 ± 0.2 H_2O of the freezable interlamellar water per lipid, in contrast with the

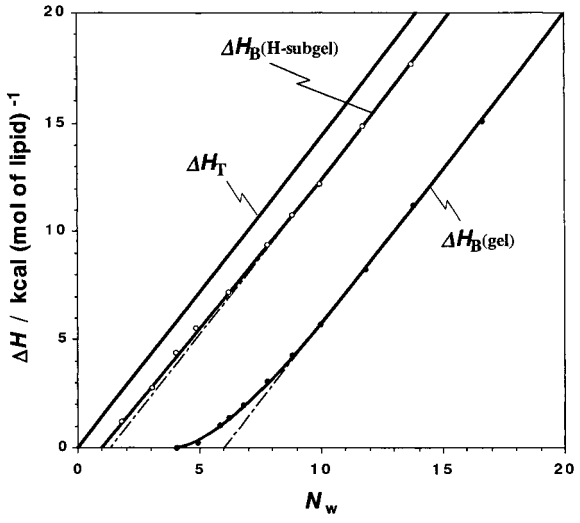

Fig. 6. Plots against N_w of ice-melting enthalpy for the bulk water, ΔH_B, per mol of lipid in DMPE–water system. ΔH_B curve for H-subgel phase is compared with that for the gel phase and also ΔH_T curve obtained by assuming that all the water added to a sample is present as the bulk water.

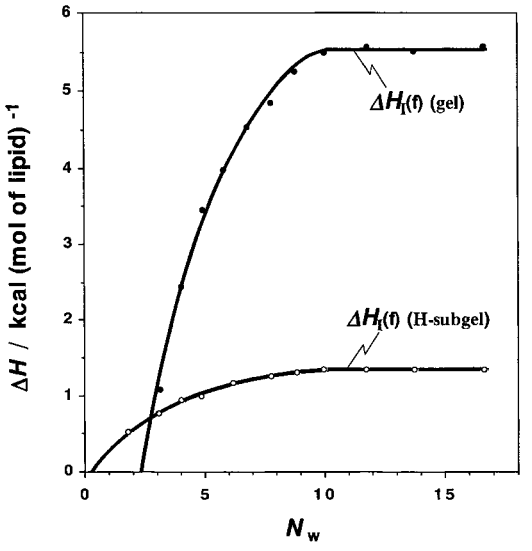

Fig. 7. Plots against N_w of ice-melting enthalpy for the freezable interlamellar water, $\Delta H_{I(f)}$, per mol of lipid in DMPE–water system. $\Delta H_{I(f)}$ curve for H-subgel phase is compared with that for the gel phase.

corresponding values of 2.3 ± 0.2 and 3.7 ± 0.2 for the fully hydrated gel phase. Accordingly, the difference in N_I ($=N_{I(nf)} + N_{I(f)}$) amounts to 4.7 ($=6.0 - 1.3$) $\pm$ 0.2 H_2O, which are composed of 2.0 ($=2.3 - 0.3$) $\pm$ 0.2 H_2O of the nonfreezable water and 2.7 ($=3.7 - 1$) $\pm$ 0.2 H_2O of the freezable interlamellar water. This accounts for a dehydration process which occurs in both the intrabilayer and interbilayer regions during periods of annealing for the conversion of the gel to H-subgel phases. Thus, 4.7 $H_2O \pm 0.2$ H_2O of water molecules per lipid present as members of the interlamellar water in the gel phase are excluded outside the bilayers, and present as the bulk water coexisting with resultant H-subgel phase. In this con-

Table 1
A summary in estimations of the number of water molecules present as nonfreezable interlamellar and freezable interlamellar waters and bulk water in H-subgel phase of DMPE–water system

Water/lipid molar ratio	The number of water molecules		
	$N_{I(nf)}$[b]/lipid	$N_{I(f)}$[c]/lipid	N_B[d]/lipid
$N_w < 0.3$	N_T[a]	0	0
$0.3 \leq N_w < 1$[e]	0.3 ± 0.2[h]	$(N_T - 0.3) \pm 0.2$	0
$0 \leq N_w < 10$	0.3 ± 0.2	$[(\Delta H_T$[f] $- \Delta H_B$[g]$)/1.436 - 0.3] \pm 0.2$	$(\Delta H_B/1.436) \pm 0.2$
$N_w \geq 10$	0.3 ± 0.2	1 ± 0.2	$(\Delta H_B/1.436) \pm 0.2$

[a] N_T is equal to N_w (lipid/water molar ratio).
[b] The number of water molecules present as nonfreezable interlamellar water.
[c] The number of water molecules present as freezable interlamellar water.
[d] The number of water molecules present as bulk water.
[e] The bulk water begins to appear at approximately $N_w = 1$.
[f] ΔH_T is equal to 1.436 N_w ($=N_T$).
[g] ΔH_B is equal to the enthalpy change per mol of lipid for deconvoluted curve IV shown in Fig. 5.
[h] The standard deviation comes from the deconvolution analysis and the polynominal curve fit used in the present study.

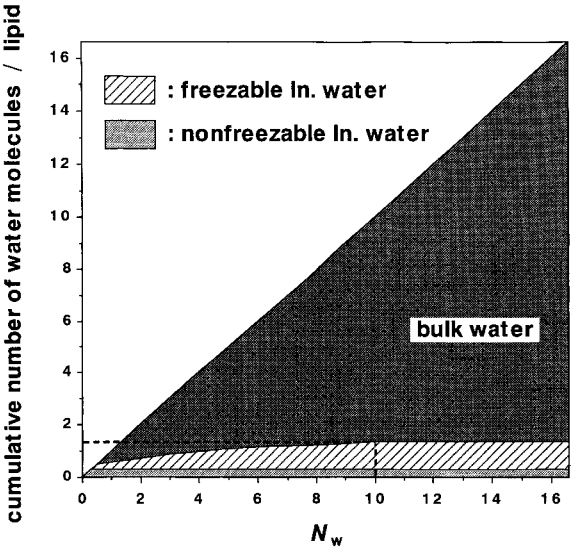

Fig. 8. Diagram of water distribution for H-subgel phase of DMPE–water system. Cumulative number of water molecules per lipid is plotted against N_w.

nection, it is necessary to consider a hydrogen bond forming property of PE molecule [13]. So, focusing on the freezable interlamellar water of approximately 1 H_2O per lipid which is left in H-subgel phase, it is suggested that adjacent bilayers of the subgel phase are linked via a hydrogen bond involving the freezable interlamellar water molecule. A similar structure has been reported for a DLPE crystal involving a molecule of acetic acid used for the crystallization [14,15]. Furthermore, focusing on almost no nonfreezable interlamellar water for H-subgel phase, it is suggested that PE molecules in an intrabilayer of the subgel phase directly combine by their intermolecular hydrogen bonds formed between the phosphate group of one molecule and the amino group of an adjacent molecule [13–15], indicating that the lipid packing is closer together for the subgel phase than for the gel phase. A closer lipid packing induces a larger contribution of the van der Waals interaction energy of the hydrocarbon chains depending on the chain–chain separation [7,16–18], so that a fairly lower enthalpy of H-subgel phase relative to the gel phase shown in Fig. 1 is induced.

References

[1] M. Kodama, H. Inoue, Y. Tsuchida, Thermochim. Acta 266 (1995) 373.
[2] H. Aoki, M. Kodama, J. Thermal Anal. 49 (1997) 839.
[3] H. Takahashi, H. Aoki, H. Inoue, M. Kodama, I. Hatta, Thermochim. Acta 303 (1997) 93.
[4] H. Chang, R.M. Epand, Biochim. Biophys. Acta 728 (1983) 319.
[5] H.H. Mantsch, S.C. Hsi, K.W. Butler, D.G. Cameron, Biochim. Biophys. Acta 728 (1983) 325.
[6] S. Mulukutla, G.G. Shipley, Biochemistry 23 (1984) 2514.
[7] D.A. Wilkinson, J.F. Nagle, Biochemistry 23 (1984) 1538.
[8] J. Silvius, P.M. Brown, T.J. O'Leary, Biochemistry 25 (1986) 4249.
[9] P.M. Brown, J. Steers, S.W. Hui, P.L. Yeagle, J.R. Silvius, Biochemistry 25 (1986) 4259.
[10] M. Kodama, H. Aoki, H. Takahashi, I. Hatta, Biochim. Biophys. Acta 1329 (1997) 61.
[11] J.F. Nagle, M.C. Wiener, Biochim. Biophys. Acta 942 (1988) 1.
[12] M. Kodama, M. Kuwabara, S. Seki, Biochim. Biophys. Acta 689 (1982) 567.
[13] J.M. Boggs, Biochim. Biophys. Acta 906 (1987) 353.
[14] H. Hauser, I. Pascher, R.H. Pearson, S. Sundell, Biochim. Biophys. Acta 650 (1981) 21.
[15] G.G. Shipley, in: D.M. Small (Ed.), Handbook of Lipid Research, Vol. 4, Plenum Press, New York, 1986, p. 97.
[16] J.F. Nagle, D.A. Wilkinson, Biophys. J. 23 (1978) 159.
[17] D.A. Wilkinson, J.F. Nagle, Biochemistry 20 (1981) 187.
[18] M. Kodama, H. Aoki, T. Miyata, Biophys. Chem. 79 (1999) 205.